Renewable Energy 154 (2020) 767–773

Contents lists available at ScienceDirect

Renewable Energy

journal homepage: www.elsevier.com/locate/renene

Gold nanoparticles mixed multiwall carbon nanotubes, supported on graphene nano-ribbons (Au-NT-G) as an efficient reduction electrode for Polymer Electrolyte Membrane fuel cells (PEMFC)

Hamid Latif [a, *], Danish Wasif [a], Saba Rasheed [a], Abdul Sattar [b], M. Shahid Rafique [c], Abdul Waheed Anwar [b], S. Zaheer [a], Syeda Ammara Shabbir [a], Ayesha Imtiaz [d], Mehwish Qutab [a], Arslan Usman [b]

[a] Department of Physics, Forman Christian College, Lahore, Pakistan
[b] Physics Department, COMSATS University Islamabad, Lahore Campus, Lahore, Pakistan
[c] Department of Physics, University of Engineering and Technology, Lahore, Pakistan
[d] Department of Chemistry, Government College University, Lahore, Pakistan

ARTICLE INFO

Article history:
Received 17 November 2019
Received in revised form
21 February 2020
Accepted 11 March 2020
Available online 17 March 2020

Keywords:
Polymer electrolyte membrane fuel cells
Graphene nano-ribbons
Multiwall carbon nanotubes
Gold nanoparticles

ABSTRACT

This research reports fabrication of three Polymer Electrolyte Membrane fuel cells (PEMFC) using composite of gold nanoparticles and nanotube graphene by varying concentration of Gold nanoparticles. The outer most layer of multiwall carbon nanotubes is un-zipped and nano ribbons of graphene are developed to attain a durable electrode. Moreover, the addition of gold nanoparticles adds benefit of better conductance over usual platinum electrodes. The effect of changing gold concentration on properties of composite material as well as fuel cell performance is investigated. The presence of gold nanoparticles and graphene nano-ribbons attached to carbon nanotubes are identified using SEM, TEM, and Raman analysis. Cyclic voltammetry analysis has showed that increase in concentration of gold nano particles improves the performance of fuel cell. EIS analysis reveled that the polarization resistance decreased by increasing the Au concentration. Thermal Gravimetric Analysis proved the thermal stability of composite material. Maximum power density of 242.29 $mWcm^{-2}$ is achieved for the highest concentration of Gold nanoparticles.

1. Introduction

With the increase in energy demand due to global population and industry requirement, qualitative research has been done to develop alternate energy systems in last two decades. Fuel to energy conversion of fossil fuel combustion systems is up to 30% but its sources are diminishing and about 70% energy of fuel is lost as heat. Over conventional energy sources, Fuel cells have advantage that the energy source is non-depleting, no harmful by product, low energy cost and do not depend on depleting sources [1].

The fuel cell system is an outstanding technique which converts chemical energy of hydrogen (fuel) into electrical energy by releasing electrons [2].

Polymer Electrolyte Membrane fuel cell has better efficiency, abundant fuel source, approximately zero emission, higher power density, quick start-up and quiet operation [3]. Hydrogen (H_2) formed by dissociation of water molecule releases an electron and transfers it to other side of fuel cell. Of many issues including degradation of membrane, exhaust of electrode in the early stages main issue is the PEM electrodes [4]. Commercially available platinum (Pt) is most common catalyst material used for the oxygen reduction reactions (ORR) at cathode [5], but due to expensive cost of platinum there is a limitation to power generation at large scale.

The selection of material for PEMFC electrode is the task that should be done while keeping some factors in mind, it must be durable, cost effective and also have improved efficiency for the transport of protons [6]. Beside these factors, thermal conductivity must also be taken into account [7,8].

To enhance the performance of fuel cell the materials used for electrode structure are very important. Monolayer graphene sheet has benefits of large surface area, better conductivity and catalytic

* Corresponding author.
E-mail address: hamidlatif@fccollege.edu.pk (H. Latif).

https://doi.org/10.1016/j.renene.2020.03.061
0960-1481/

activity. Because of these outstanding characteristics graphene has become a promising candidate for applications in PEM fuel cell [9]. Graphene also has ability to permit fast transport of protons and selective separation of ions. PEM fuel cell allows to transfer proton and blocks the water molecule. So it is possible to transmit only hydrogen ions towards the PEM membrane by introducing graphene along with metallic nanoparticles in catalytic process.

PEM fuel cells suffer due to high cost of electrodes and membrane [10,11]. This research project reports an attempt to fabricate an efficient PEM fuel cell using composite of graphene nanoribbons with varied concentrations of gold nanoparticles as a reduction electrode. Three PEM fuel cells were fabricated with varied concentrations of gold nanoparticles. The materials used here are cheap and their synthesis technique is also simple.

2. Experimental section

Fig. 1 schematically shows the exfoliation of MWCNTs into graphene nano ribbons along with un-zipped CNTs. It also describes the formation of Au nano particles decorated nano tube graphene composite for the application in PEM fuel cell.

Nano ribbons of graphene were synthesized by exfoliation of MWCNTs followed by the pretreatment of strong acid and dried at high temperature and low vacuum in furnace to avoid damaging the combustible carbon content. Briefly, 0.5 g of MWCNTs were dissolved in 20 ml concentrated H_2SO_4 and continuously stirred for 48 h. Then, 2.5g of $KMnO_4$ was slowly added to the ongoing reaction (pH < 3). Then, 5 ml of H_2O_2 was added dropwise in an ice bath. The solution was stirred at 65 °C for 2 h and centrifuged at 8000 rpm. The pH of 4 was achieved by several times washing residual with 5% hydrochloric acid (HCl) solution mixed with water. The thick residual was dried at 900 °C in vacuum furnace in ammonia environment [12].

For gold nanoparticles, 20 ml of 1 mM chloroauric acid tetrahydrate ($HAuCl_4$) solution was heated at 400 °C. Then, 2 ml of 34 mM TCD solution was added and stirred for 20 min until the color of solution begins to change to purple. Heat was then removed and solution was allowed to cool, the color transition takes place from purple to red wine in this step [13].

The NT-G ink is formed by addition of 30 mg NT-G and 0.3g of SDS to 30 ml of deionized water and dip sonicated for 75 min. The resultant solution was centrifuged at 7000 revolutions per minute (rpm) for 30 min [14].

The NT-G ink was then put in a beaker and gold nanoparticles were added in it and dispersed using dip sonicator. Three different samples were prepared with different concentrations of gold nanoparticles. The ratio of Au-NP to NT-G is 0:5, 1:5, 1:2.5, 1:1.6 later named as 0% Au-NT-G, 20% Au-NT-G, 40% Au-NT-G, and 60% Au-NT-G. Gold nanoparticle solution was added in 4 ml of NT-G solution. The beaker was stirred and sonicated for an hour. The homogenous solution was centrifuged at 7000 rpm for 30 min. All prepared three samples were then deposited using spin coater at 3000 rpm on Toray carbon sheet of size 10 mm × 10 mm.

The present study provides a detail account of how the variations in concentration of gold nano particles affect the characteristics of synthesized nano composites and their corresponding behavior for PEM fuel cell as a catalyst. After fabrication the samples are analyzed by characterization techniques like thermal gravimetric analysis (TGA), transmission electron microscopy (TEM), scanning electron microscopy, Raman spectroscopy and cyclic voltammetry (CV). Finally, all the samples were tested in PEM fuel cell assembly for their performance.

3. Analysis

3.1. Structural morphological and elemental analysis

To reflect the surface morphology and structure of composite

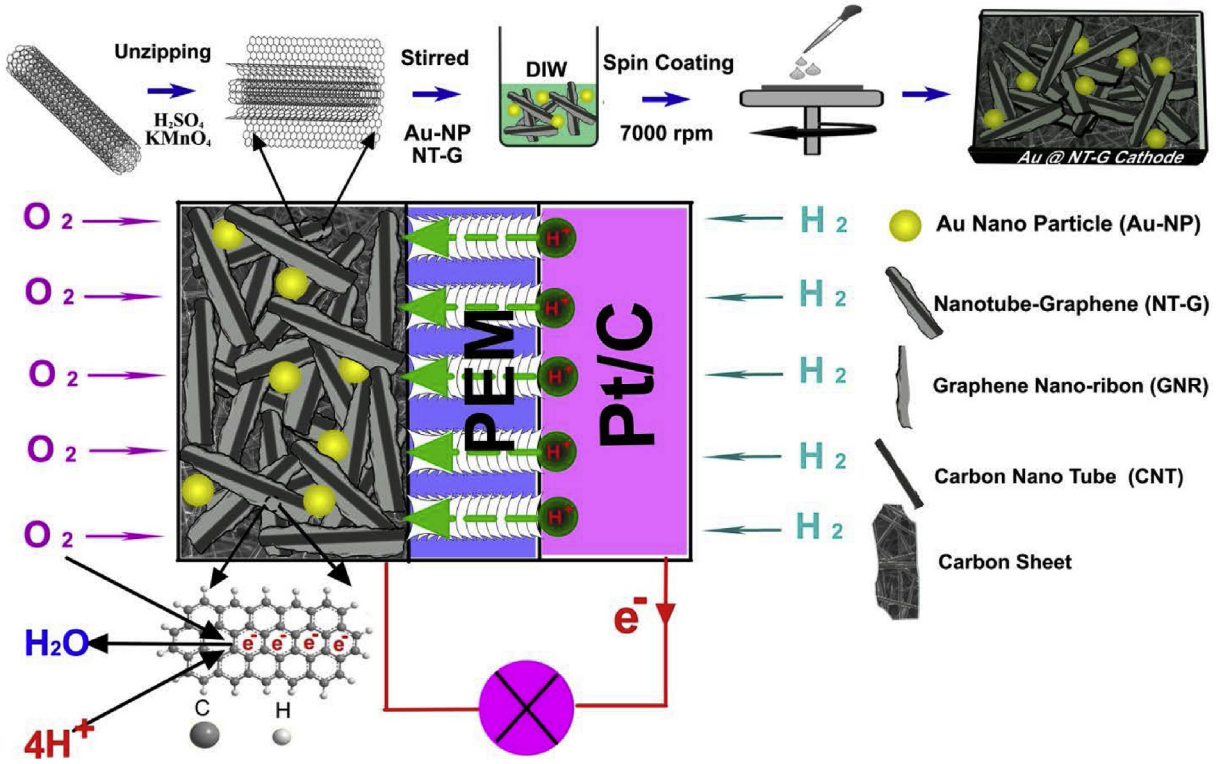

Fig. 1. Schematic diagram of PEM fuel cell. Synthetic route of Au-NT-G.

SEM and TEM analysis were carried out respectively. SEM image in Fig. 1 (a) shows the surface morphology of thin film of Au-NT-G composite spin coated over carbon sheet. This image shows the fibrous structure of carbon sheet. For further investigation selected area of this micrograph is magnified. The magnified images shown in Fig. 1b and (c) reveal that CNTs are randomly dispersed on fibrous structure of carbon sheet. The partially un-zipped CNTs have formed ribbon like graphene sheets which are attached to remaining CNTs. The presence of gold nanoparticles is not confirmed by SEM analysis.

The TEM micrograph of composite shown in Fig. 1d proves the existence of gold nanoparticles, graphene nano-ribbons, nano tube graphene and CNTs. The spherical shaped black dots represent the gold nano particles, strands like structures represent CNTs. Both CNTs and gold nano particles are dispersed on ribbon like graphene nano-sheets [15]. EDS spectra in Fig. 2g shows elemental analysis of the composite and Au and C peek are evident in the spectra.

Fig. 2e displays combined Raman spectra of all three samples to observe the presence of bands in the carbon based materials and to measures disorder due to its high sensitivity towards changes in structure of carbonaceous materials. The main aspect of Raman spectra is D and G-band in carbon materials. D- Band (defect band) is attributed to A_{1g}-zone boundary mode due to the disorder in sp^2 hybridized structure has very low intensity in all Au-NT-G samples. G-band due to C—C stretching mode is present in all carbon based materials. In present case, G-band due to the E_{2g} of group theory at Γ-point was present at 1582.8 cm^{-1}, 1581.8 cm^{-1}, 1581.9 cm^{-1} and 1584.6 cm^{-1} for NT-G, 20% Au-NT-G, 40% Au-NT-G and 60% Au-NT-G respectively. Using these values of G- Band, graphene was found to be monolayer in each case. The double resonant 2D Raman peak due to second phonon scattering was present at 2707 cm^{-1}, 2708 cm^{-1} and 2723 cm^{-1} with an increased intensity for higher concentration of gold nanoparticles. The peak for gold nanoparticles was present at 734 cm^{-1}.

Fig. 2f shows the Raman spectra for 20% Au-NT-G, 40% Au-NT-G, and 60% Au-NT-G. It allows to observe the presence of bands in the carbon based materials and to measures disorder due to its high sensitivity towards changes in structure of carbonaceous materials. The G (graphitic), D (defect) and 2D (second order harmonic to D) bands are visible. The main aspect of raman spectra is D and G-band in carbon materials. D- Band (defect band) at 1365.8 cm^{-1} is attributed to A_{1g}-zone boundary mode due to the disorderness in sp^2 hybridized structure has very low intensity in all Au-NT-G samples. G-band due to C—C stretching mode is present in all carbon based materials. In present case, G-band due to the E_{2g} (raman active mode) of group theory at Γ-point was present at 1583.4 cm^{-1}, 1581.7 cm^{-1} and 1581.1 cm^{-1} for 20% Au-NT-G, 40% Au-NT-G and 60% Au-NT-G respectively. Using these values of G-Band, graphene was found to be monolayer in each case. The double resonant 2D raman peak due to second phonon scattering was present at 2709.4, 2714.3 and 2725.2 cm^{-1} for 20% Au-NT-G, 40% Au-NT-G and 60% Au-NT-G respectively. The peak for Au-NP

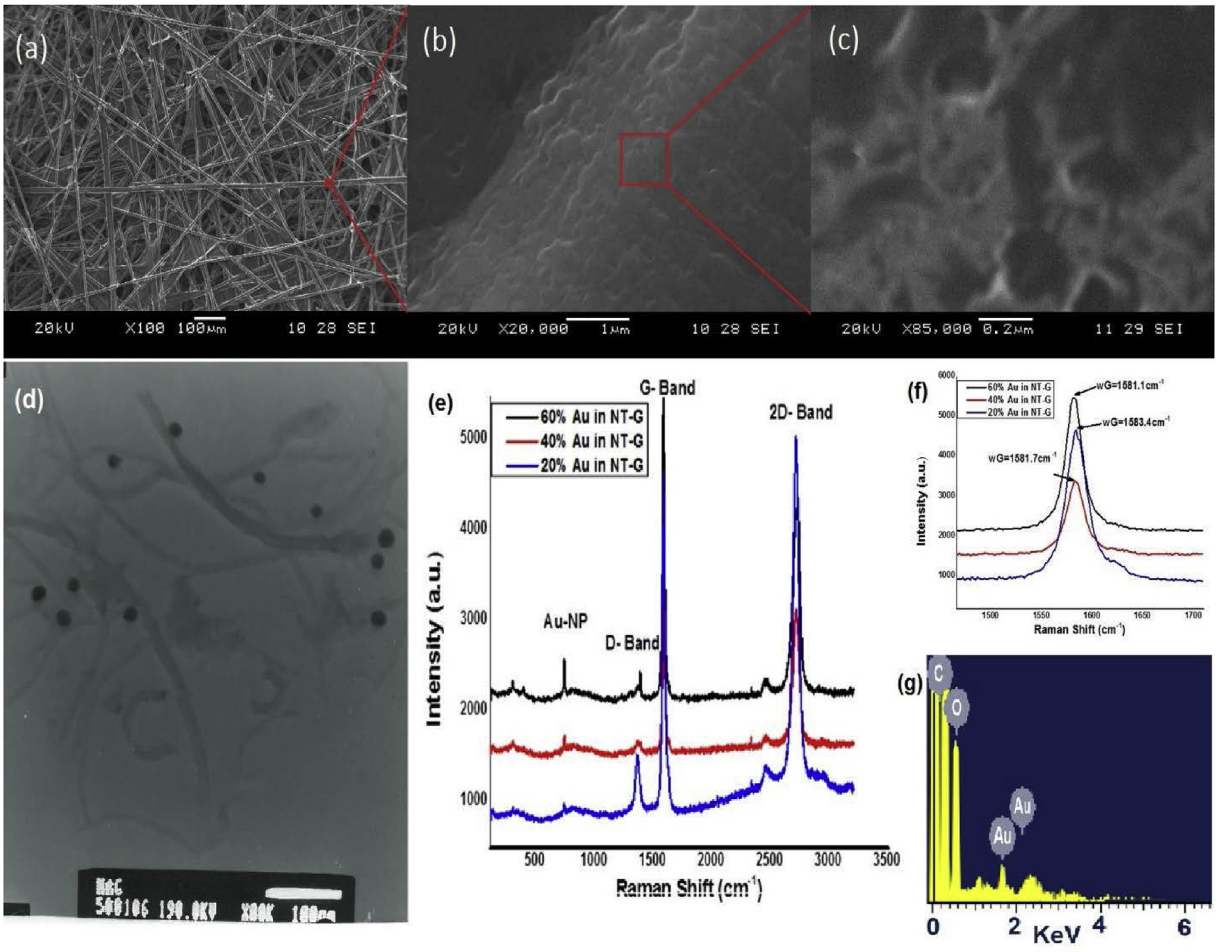

Fig. 2. (a, b, c): SEM images of Au-NT-G composite thin film on carbon sheet at different magnifications. **(d)**TEM image of Au-NT-G composite **(e)** Combined graph for Raman spectra of sample 1, 2 and 3. **(f)** G- Band location in Raman Spectra (g) EDS spectra of Au-NT-G.

was present at 730.6 cm^{-1} with an increased intensity for higher concentration of Au-NP [16–19].

3.2. Cyclic voltammetry

Cyclic voltammetry diagnostic was performed to study the electrochemical behavior of Au-NT-G samples in 0.1 M $HClO_4$ electrolyte solution with platinum electrode as reference electrode and catalyst solution was deposited on glassy carbon electrode (GC). Our main concern was to study the electrochemical properties of composite after the addition of gold as without gold, NT-G complex have been observed before [12]. The electrochemical HOR and ORR activity was evaluated from the CV curves for all the three samples shown in Fig. 3. The peaks for oxidation reduction reactions showed that the sample with 60% Au concentration has better electrochemical activity while sample with 0% Au-NP concentrations has shown worse electrochemical behavior among all the samples. Also, the cathodic current was found to be increased as the concentration of Au nanoparticles was increased; a clear indication towards increase in electrocatalytic activity in the oxygen reduction reaction.

The reduction and oxidation peaks current for NT-G, 20% Au-NT-G, 40% Au-NT-G and 60% Au-NT-G were at −0.5 μA, 0.496 μA, 6.446 μA, 8.738 μA and 0.863 μA, 1.933 μA, 4.039 μA and 8.069 μA respectively.

The D band related to defects in Raman spectra and TEM micrograph confirms the presence of defects in structure of graphene. Recent research has shown that the defect rich carbon materials can catalyze oxidation reduction reaction effectively in both acidic and alkaline electrolytes [20]. Graphene nano-ribbons (GNRs) are promising material for catalyst due to numerous defects along edges and larger aspect ratio [21]. The method we have used to unzip the MWCNTs creates zig-zag type carbon along the edges of graphene nano-ribbons [22]. CNTs prevent stacking of graphene nano-ribbons in catalyst layer. Carbon sheet introduced in catalyst layer further separates GNRs and CNTs and this facilitates the transport of mass in catalyst layer to confirm use of defects. As a result, stable and efficient catalytic activity proceeds [23].

Results obtained from CV curves are tabulated in Table 1. It is observed that enhancement in catalytic activity depends on concentration of gold nano particles. Gold catalysts are highly active towards ORR [24]. We have used gold nanoparticles (Au-NP) along with nano tube graphene and un-zipped MWCTs in catalyst layer. It is observed from the CV analysis increase in concentration of gold nanoparticles leads to enhancement in electro-catalytic activity of electrode. This is because metal doped graphene materials increases the active surface area of electrodes [25]. So Au-NT-G composite material holds great potential for developing novel electrodes for PEM fuel cells.

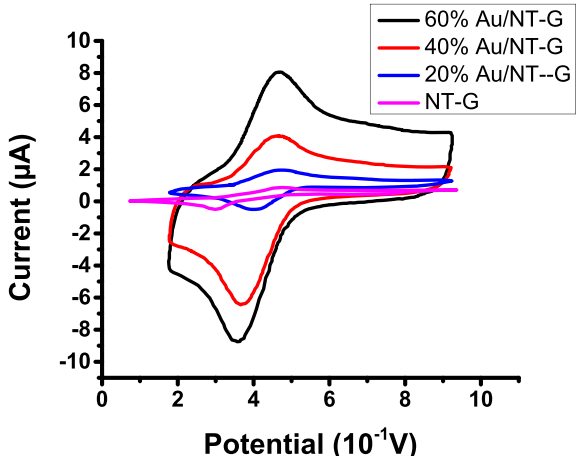

Fig. 3. Cyclic voltammograms for 20% Au-NT-G, 40% Au-NT-G, and 60% Au-NT-G.

3.3. Electrochemical impedance spectra (EIS) analysis

Fig. 4 shows the Nyquist plot for all the samples. It can be seen from the plot that diameter of impedance curves have decreased by increasing the percentage of the Au particle in the composite.

*E*lectrolyte resistance (R_s), coating resistance (R_f), and charge transfer resistance (R_{ct}) are evaluated and shown in Table 2.The polarization resistance (Rp) which is calculated by the adding charge transfer and coating resistant seems to decrease by increasing the percentage of the Au nano-particles. It can be seen from Table 2 that the sample without Au has maximum polarization resistance 31505 Ωcm^2. The decrease in the polarization resistance is due the improved conductivity of the composite by increasing the Au concentration.

3.4. Cell performance

After CV characterization all the three samples were assembled in the membrane electrode assembly (MEA) to evaluate performance in actual PEM fuel cell. The actual activity of electrode is determined from its PEM fuel cell performance curves. The polarization curve, a plot of cell voltage and power density versus current density, shown in Fig. 4 reflects the performance of Au-NT-G composite based PEM fuel cell.

It is observed from the polarization curves shown in Fig. 5 that voltage drawn increases as the concentration of gold nano particles increases. The similar trend is observed for the power density. 60% Au-NT-G sample with maximum concentration of gold nano particles exhibits best polarization curve with highest peak power density while 40% Au-NT-G and 20% Au-NT-G samples show relatively low performances due to lower concentrations of gold nano particles. The power density after attaining the peak value declines due to worst oxygen transport in catalyst layer. The performance decay is relatively small for 60% Au-NT-G sample. It can be attributed to increased concentration of gold nano particles which increases the active surface area of electrode. The increase in reactive surface area improves the catalytic cavity [26].

The values of maximum power density for all three samples are 62.01 $mWcm^{-2}$, 136.25 $mWcm^{-2}$ and m242.29 Wcm^{-2} for 20% Au/NT-G, 40% Au-NT-G and 60% Au-NT-G respectively. It is obvious from Fig. 6 that 60%Au-NT-Gsample with maximum concentration of gold has highest value of maximum power density as compared to other two samples.

PEM fuel cell based on Pt/C catalyst showed maximum power density of 178 mW/cm^{-2} as conventional Pt/C electrocatalyst has certain limitations like high cost and degradation therefore other materials have also being used for catalyst. Alloys based on different metals are also being used as catalyst. RhAu alloy nanoparticles have shown good catalytic activity [31]. FePd@Pd electrocatalyst showed stability and activity comparable to that of commercially used Pt/C. AuCu and AuPd are also being used as electrocatalyst [32]. Composite of Pd–Co alloy nanoparticles and nitrogen doped reduced graphene oxide has shown great potential for application in PEM fuel cell as anode electrocatalyst [33].

PEM fuel cell based on MWCNTs-platinum nanocomposite catalyst showed peak power density of 156 mW/cm^{-2} whereas peak power density of 247 mW/cm^{-2} was achieved using platinum/graphene nanoplatelets [34–36].

By replacing conventional Pt/C by composite of gold nanoparticles mixed multiwall carbon nanotubes supported on

Table 1
Results of CV.

Sample Composition	Oxidation Potential (V)	Corresponding Current (+μA)	Reduction Potential (V)	Corresponding Current (-μA)
0% Au-NT-G	0.465	0.863	0.29	−0.5
20% Au-NT-G	0.469	1.933	0.403	0.496
40% Au-NT-G	0.466	4.039	0.369	6.446
60% Au-NT-G	0.467	8.069	0.361	8.738

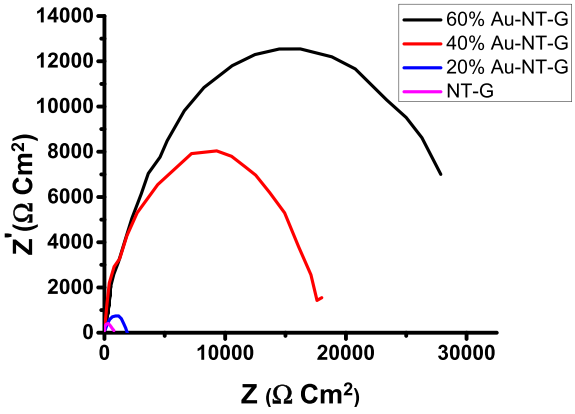

Fig. 4. Nyquist plots for EIS data.

Table 2
EIS analysis data.

Sample	R_s (Ωcm^2)	R_f (Ωcm^2)	R_{ct} (Ωcm^2)	R_p (Ωcm^2)
60% Au-NT-G	5.49	5.22	605	610.22
40% Au -NT-G	5.83	17.96	1640	1657.
20% Au-NT-G	5.21	112.21	17580	17692.21
NT-G	6.32	291.31	31215	31506

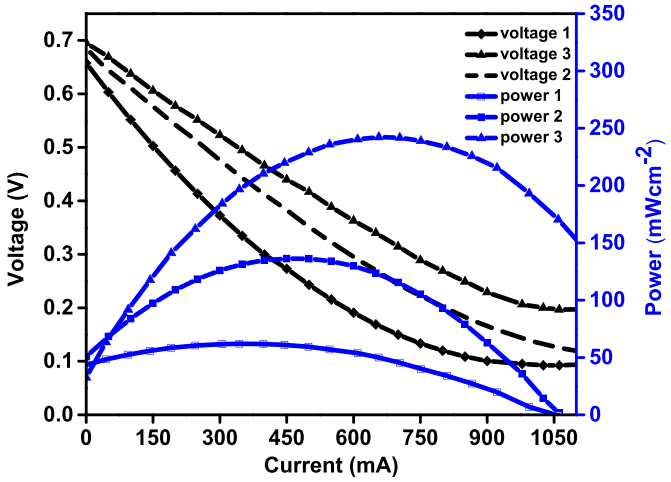

Fig. 5. Polarization curves of 20% Au-NT-G, 40% Au-NT-G, and 60% Au-NT-G.

graphene nano-ribbons (Au-NT-G), maximum power density of 242.29 Wcm^{-2} is reported in this research, which is clearly more than maximum power density of the fuel cells discussed above.

3.5. Thermal gravimetric analysis

In order to determine the stability of composite over a wide range of temperature, thermal gravimetric analysis was performed.

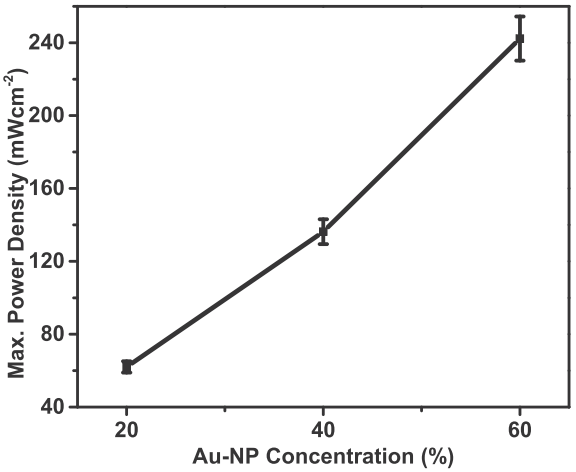

Fig. 6. Comparative maximum power density.

From the observation based on weight profiles of TGA as a function of variation in temperature as shown in Fig. 7, it was concluded that the Au-NT-G samples have no water molecules as there was no weight loss and the decomposition of carbon takes place above 500 °C for all samples. The overall stability of Au-NT-G composite was better than the approaches used before [27–30] as weight loss occurs at higher temperature which might be due to the presence of CNTs. The stability of our composite with 20% Au in NT-G was better in all but it decreases with the further addition of gold nanoparticles.

Although this type of fuel cell operates at low temperatures but TGA analysis shows the composite material do not decompose and remains stable at 500 °C. So this fuel cell can operate at relatively high temperature.

The structure stability of this fuel cell system is better due to the presence of carbon nanotubes and graphene. Graphene and carbon nanotubes both exhibit better mechanical strength which can contribute towards better structural stability [37]. It can be seen from SEM and TEM micrographs that carbon nanotubes are dispersed on fibrous carbon sheet. Partially un-zipped carbon nanotubes that have formed ribbon like structure of graphene are attached to the remaining carbon nanotubes. The carbon nanotubes which are entangled in spaces between graphene nano ribbons and gold nanoparticles will enhance the strength and stability [38].

4. Conclusion

In this research we fabricated hybrid electrocatalyst using gold nanoparticles and nano tube graphene. Three different samples were prepared with varying concentrations of gold nanoparticles. These samples were then analyzed by different characterization techniques. Scanning Electron Microscopy (SEM) exposed presence of randomly dispersed CNTs on fibrous carbon sheet along with ribbon like structure of graphene. Transmission Electron Microscopy (TEM) confirmed the existence of gold nanoparticles. Raman

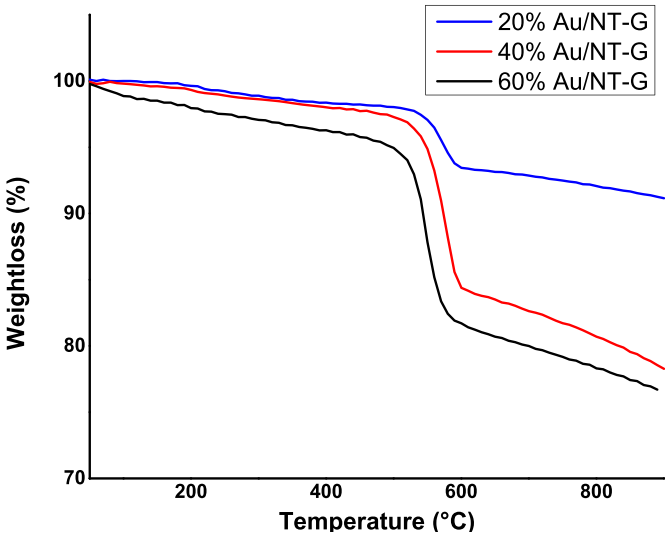

Fig. 7. Combined graph of TGA analysis for 20% Au-NT-G, 40% Au-NT-G, and 60% Au-NT-G sample.

Spectroscopy also showed presence of gold nanoparticles peak at 1358 cm-1 in all three samples. Raman spectra showed the peaks of all the relevant materials. Raman calculations also confirmed the growth of monolayer graphene. Cyclic Voltammetry analysis revealed that prepared electrode of Au-NT-G has improved cathodic current of 8.7 μA and reduction potential of 0.36V as compared to previously reported for NT-G electrode. Polarization resistance has decreased by increasing the Au concentration. Polarization curves have proved that cell performance is dependent on concentration of gold nano particles and highest power density of 242.29 Mw/cm^{-2} is achieved for 60% Au-NT-G sample. As compared to conventional Pt or CNT based electrode gold nanoparticles decorated NT-G has shown a great potential. TGA analysis proved that prepared material has no weight loss at operating temperatures of fuel cell. But still there is a room for further research to achieve an efficient, durable and long lasting electrode suitable for harsh working environment.

CRediT authorship contribution statement

Hamid Latif: Conceptualization, Methodology, Investigation, Writing - original draft, Supervision. **Danish Wasif:** Methodology. **Saba Rasheed:** Investigation, Validation. **Abdul Sattar:** Resources. **M. Shahid Rafique:** Resources. **Abdul Waheed Anwar:** Resources. **S. Zaheer:** Formal analysis. **Syeda Ammara Shabbir:** Resources. **Ayesha Imtiaz:** Formal analysis. **Mehwish Qutab:** Formal analysis. **Arslan Usman:** Resources.

Appendix A. Supplementary data

Supplementary data to this article can be found online at https://doi.org/10.1016/j.renene.2020.03.061.

References

[1] L. Carrette, K.A. Friedrich, U. Stimming, Fuel cells–fundamentals and applications, Fuel Cell. 1 (2001) 5–39.
[2] M. Beltrán-Gastélum, M.I. Salazar-Gastelum, R.M. Felix-Navarro, S. Perez-Sicairos, E.A. Reynoso-Soto, S.W. Lin, J.R. Flores-Hernandez, T. Romero-Castanon, I.L. Albarran-Sanchez, F. Paraguay-Delgado, Evaluation of PtAu/MWCNT (Multiwalled Carbon Nanotubes) electrocatalyst performance as cathode of a proton exchange membrane fuel cell, Energy 109 (2016) 446–455.
[3] J. Zhu, J. Tan, Q. Pan, Z. Liu, Q. Hou, Effects of Mg2+ contamination on the performance of proton exchange membrane fuel cell, Energy 189 (2019) 116135.
[4] B.C. Steele, A. Heinzel, Materials for fuel-cell technologies, Mater. Sustain. Energy (2011) 224–231.
[5] D.C. Higgins, D. Meza, Z. Chen, Nitrogen-doped carbon nanotubes as platinum catalyst supports for oxygen reduction reaction in proton exchange membrane fuel cells, J. Phys. Chem. C 114 (2010) 21982–21988.
[6] W.R. Daud, R.E. Rosli, E.H. Majlan, S.A. Hamid, R. Mohamed, T. Husaini, PEM fuel cell system control: a review, Renew. Energy 113 (2017) 620–638.
[7] O.S. Burheim, Review: PEMFC materials' thermal conductivity and influence on internal temperature profiles, ECS Trans. 80 (2017) 509–525.
[8] S.M. Haile, Fuel cell materials and components, Acta Mater. 51 (2003) 5981–6000.
[9] E. Arici, B.Y. Kaplan, A.M. Mert, S.A. Gursel, S. Kinayyigit, An effective electrocatalyst based on platinum nanoparticles supported with graphene nanoplatelets and carbon black hybrid for PEM fuel cells, Int. J. Hydrogen Energy 44 (2019) 14175–14183.
[10] D. He, H. Tang, Z. Kou, M. Pan, X. Sun, J. Zhang, S. Mu, Engineered graphene materials: synthesis and applications for polymer electrolyte membrane fuel cells, Adv. Mater. 29 (2017) 1601741.
[11] B. Saner, F. Okyay, Y. Yürüm, Utilization of multiple graphene layers in fuel cells. 1. An improved technique for the exfoliation of graphene-based nanosheets from graphite, Fuel 89 (2010) 1903–1910.
[12] Y. Li, W. Zhou, H. Wang, L. Xie, Y. Liang, F. Wei, et al., An oxygen reduction electrocatalyst based on carbon nanotube–graphene complexes, Nat. Nanotechnol. 7 (2012) 394.
[13] M. Chen, C. Hou, D. Huo, J. Bao, H. Fa, C. Shen, An electrochemical DNA biosensor based on nitrogen-doped graphene/Au nanoparticles for human multidrug resistance gene detection, Biosens. Bioelectron. 85 (2016) 684–691.
[14] E.S. Ates, S. Kucukyildiz, H.E. Unalan, Zinc oxide nanowire photodetectors with single-walled carbon nanotube thin-film electrodes, ACS Appl. Mater. Interfaces 4 (2012) 5142–5146.
[15] R. Nandan, G.K. Goswami, K.K. Nanda, Direct synthesis of Pt-free catalyst on gas diffusion layer of fuel cell and usage of high boiling point fuels for efficient utilization of waste heat, Appl. Energy 205 (2017) 1050–1058.
[16] R.G. Bai, K. Muthoosamy, M. Zhou, M. Ashokkumar, N.M. Huang, S. Manickam, Sonochemical and sustainable synthesis of graphene-gold (G-Au) nanocomposites for enzymeless and selective electrochemical detection of nitric oxide, Biosens. Bioelectron. 87 (2017) 622–629.
[17] S.Y. Chen, J.J. Mock, R.T. Hill, A. Chilkoti, D.R. Smith, A.A. Lazarides, Gold nanoparticles on polarizable surfaces as Raman scattering antennas, ACS Nano 4 (2010) 6535–6546.
[18] L.M. Malard, M.A. Pimenta, G. Dresselhaus, M.S. Dresselhaus, Raman spectroscopy in graphene, Phys. Rep. 473 (2009) 51–87.
[19] A.C. Ferrari, Raman spectroscopy of graphene and graphite: disorder, electron–phonon coupling, doping and nonadiabatic effects, Solid State Commun. 143 (2007) 47–57.
[20] M.R. Benzigar, S. Joseph, H. Ilbeygi, D.H. Park, S. Sarkar, G. Chandra, et al., Highly crystalline mesoporous C60 with ordered pores: a class of nanomaterials for energy applications, Angew. Chem. 130 (2018) 578–582.
[21] C. Tang, Q. Zhang, Nanocarbon for oxygen reduction electrocatalysis: dopants, edges, and defects, Adv. Mater. 29 (2017) 1604103.
[22] A.L. Elías, A.R. Botello-Méndez, D. Meneses-Rodríguez, V. Jehová González, D. Ramírez-González, L. Ci, et al., Longitudinal cutting of pure and doped carbon nanotubes to form graphitic nanoribbons using metal clusters as nanoscalpels, Nano Lett. 10 (2009) 366–372.
[23] J. Shui, M. Wang, F. Du, L. Dai, N-doped carbon nanomaterials are durable catalysts for oxygen reduction reaction in acidic fuel cells, Sci. Adv. 1 (2015), e1400129.
[24] V. Mazumder, Y. Lee, S. Sun, Recent development of active nanoparticle catalysts for fuel cell reactions, Adv. Funct. Mater. 20 (2010) 1224–1231.
[25] A. Marinoiu, M. Raceanu, E. Carcadea, A. Pantazi, R. Mesterca, O. Tutunaru, S. Nica, D. Bala, M. Varlam, M. Enachescu, Noble metal dispersed on reduced graphene oxide and its application in PEM fuel cells, in: Electrocatalysts for Fuel Cells and Hydrogen Evolution: Theory to Design 69, 2018.
[26] N. Jha, R.I. Jafri, N. Rajalakshmi, S. Ramaprabhu, Graphene-multi walled carbon nanotube hybrid electrocatalyst support material for direct methanol fuel cell, Int. J. Hydrogen Energy 36 (2011) 7284–7290.
[27] P. Kar, S. Sardar, B. Liu, M. Sreemany, P. Lemmens, S. Ghosh, S.K. Pal, Facile synthesis of reduced graphene oxide–gold nanohybrid for potential use in industrial waste-water treatment, Sci. Technol. Adv. Mater. 17 (2016) 375–386.
[28] M. Kwak, S. Lee, D. Kim, S.K. Park, Y. Piao, Facile synthesis of Au-graphene nanocomposite for the selective determination of dopamine, J. Electroanal. Chem. 776 (2016) 66–73.
[29] G. Darabdhara, M.A. Amin, G.A. Mersal, E.M. Ahmed, M.R. Das, M.B. Zakaria, et al., Reduced graphene oxide nanosheets decorated with Au, Pd and Au–Pd bimetallic nanoparticles as highly efficient catalysts for electrochemical hydrogen generation, J. Mater. Chem. 3 (2015) 20254–20266.
[30] J. Li, H. Feng, J. Li, Y. Feng, Y. Zhang, J. Jiang, D. Qian, Fabrication of gold nanoparticles-decorated reduced graphene oxide as a high performance electrochemical sensing platform for the detection of toxicant Sudan I, Electrochim. Acta 167 (2015) 226–236.
[31] H. Li, L. Luo, P. Kunal, C.S. Bonifacio, Z. Duan, J.C. Yang, G. Henkelman, Oxygen reduction reaction on classically immiscible bimetallics: a case study of RhAu,

J. Phys. Chem. C 122 (2018) 2712–2716.
[32] J.A. Trindell, Z. Duan, G. Henkelman, R.M. Crooks, Well-defined nanoparticle electrocatalysts for the refinement of theory, Chem. Rev. (2019).
[33] P. Chandran, A. Ghosh, S. Ramaprabhu, High-performance Platinum-free oxygen reduction reaction and hydrogen oxidation reaction catalyst in polymer electrolyte membrane fuel cell, Sci. Rep. 8 (2018) 1–11. ++]]\ 6.
[34] T. Ioroi, Z. Siroma, S.I. Yamazaki, K. Yasuda, Electrocatalysts for PEM fuel cells, Adv. Energy Mater. 9 (2019) 1801284.
[35] C. Gupta, P.H. Maheshwari, S.R. Dhakate, Development of multiwalled carbon nanotubes platinum nanocomposite as efficient PEM fuel cell catalyst, Mater. Renew. Sustain. Energy 5 (2016) 2.
[36] E. Arici, B.Y. Kaplan, A.M. Mert, S.A. Gursel, S. Kinayyigit, An effective electrocatalyst based on platinum nanoparticles supported with graphene nanoplatelets and carbon black hybrid for PEM fuel cells, Int. J. Hydrogen Energy 4 (2019) 14175–14183.
[37] Z. Yin, J. Zhu, Q. He, X. Cao, C. Tan, H. Chen, H. Zhang, Graphene-based materials for solar cell applications, Adv. Energy Mater. 4 (2014) 1300574.
[38] X. Liu, C. Wang, B. Cai, X. Xiao, S. Guo, Z. Fan, L. Liao, Rational design of amorphous indium zinc oxide/carbon nanotube hybrid film for unique performance transistors, Nano Lett. 12 (2012) 3596–3601.